Indirect determination of the strange nucleon form factors from lattice QCD ☆

P.E. Shanahan[a,*], R. Horsley[b], Y. Nakamura[c], D. Pleiter[d,e], P.E.L. Rakow[f], G. Schierholz[g], H. Stüben[h],
A.W. Thomas[a], R.D. Young[a], J.M. Zanotti[a]

[a]*ARC Centre of Excellence in Particle Physics at the Terascale and CSSM, School of Chemistry and Physics, University of Adelaide, Adelaide SA
5005, Australia*
[b]*School of Physics and Astronomy, University of Edinburgh, Edinburgh EH9 3JZ, UK*
[c]*RIKEN Advanced Institute for Computational Science, Kobe, Hyogo 650-0047, Japan*
[d]*JSC, Forschungzentrum Jülich, 52425 Jülich, Germany*
[e]*Institut für Theoretische Physik, Universität Regensburg, 93040 Regensburg, Germany*
[f]*Theoretical Physics Division, Department of Mathematical Sciences, University of Liverpool, Liverpool L69 3BX, UK*
[g]*Deutsches Elektronen-Synchrotron DESY, 22603 Hamburg, Germany*
[h]*Regionales Rechenzentrum, Universität Hamburg, 20146 Hamburg, Germany*

Abstract

The strange contribution to the electric and magnetic form factors of the nucleon is determined at a range of discrete values of Q^2 up to 1.4 GeV^2. This is done by combining recent lattice QCD results for the electromagnetic form factors of the octet baryons with experimental determinations of those quantities. The most precise result is a small negative value for the strange magnetic moment: $G_M^s(Q^2 = 0) = -0.07 \pm 0.03 \, \mu_N$. At larger values of Q^2 both the electric and magnetic form factors are consistent with zero to within 2-sigma.

Keywords: Strangeness, Electromagnetic form factors, Lattice QCD, Chiral symmetry, Extrapolation

1. Introduction

A quantitative determination of the contribution of non-valence flavour quarks to nucleon observables remains a fundamental challenge of hadronic physics. Since such contributions must arise entirely through interactions with the vacuum, their sign and magnitude provide key information regarding the nonperturbative structure of the nucleon; their determination within nonperturbative QCD constitutes a test of a level of importance comparable to that of the Lamb shift for QED. Strange quarks, as the lightest sea-only flavour, are expected to play the largest role.

Recent years have seen extensive experimental efforts directed at measuring strangeness in the nucleon. The strange electromagnetic form factors in particular have been determined from experiments at JLab (G0, HAPPEX) [1–7], MIT-Bates (SAMPLE) [8, 9], and Mainz (A4) [10–12]. Probing a range of values of Q^2 up to ≈ 0.94 GeV^2, the combined data sets constrain the strange contribution to the nucleon form factors to be less than a few percent but are consistent with zero to within 2-sigma [13]. The status of the strange form factors from theory is less clear; predictions from various quark models cover a very broad range of values [14–19], and the large computational cost of all-to-all propagators has so far limited direct lattice QCD studies to large pion masses and single volumes [20, 21].

Here we determine the strangeness contributions to the nucleon electromagnetic form factors indirectly from lattice QCD. Under the assumption of charge symmetry, one can combine experimental measurements of the nucleon form factors with lattice QCD determinations of the connected (or 'valence' quark) contributions to deduce the disconnected (or 'sea' quark) components [22]. This method has been applied previously to determine the strange magnetic form factor at $Q^2 = \{0, 0.23\}$ GeV^2 [23, 24] and the strange electric form factor at $Q^2 = 0.1$ GeV^2 [25] from quenched lattice QCD studies. We extend that work to six discrete values of the momentum transfer using the results of new dynamical 2 + 1–flavour lattice QCD simulations from the CSSM/QCDSF/UKQCD Collaborations [26, 27].

---

2. Strange form factors

Our calculation is based on the recent lattice investigation and analysis reported in Refs. [26, 27]. Those studies determine the connected quark contributions to the electric and magnetic form factors of the outer-ring octet baryons using $2 + 1$–flavour lattice QCD simulations extrapolated to infinite volume and to the physical pseudoscalar masses. That extrapolation is performed using a formalism based on connected chiral perturbation theory [28, 29].

The extraction of the strange electromagnetic form factors from the extrapolated lattice results follows the procedure introduced in Refs. [30, 31]. Under the assumption of charge symmetry, which is an exact symmetry of QCD if one neglects QED and the light quark mass difference (i.e., assuming $m_u = m_d$), one may express the electromagnetic form factors of the proton and neutron as [22]

$$p = e^u u^p + e^d d^p + O_N, \qquad (1)$$

$$n = e^d u^p + e^u d^p + O_N. \qquad (2)$$

Here, p and n denote the physical (electric or magnetic) form factors of the proton and neutron and u^p and d^p represent the connected u and d quark contributions to the proton form factor. The disconnected quark loop term, O_N, may be decomposed into individual quark contributions:

$$O_N = \frac{2}{3} {}^\ell G^u - \frac{1}{3} {}^\ell G^d - \frac{1}{3} {}^\ell G^s, \qquad (3)$$

$$= \frac{{}^\ell G^s}{3} \left(\frac{1 - {}^\ell R_d^s}{{}^\ell R_d^s} \right), \qquad (4)$$

where charge symmetry has been used to equate ${}^\ell G^u = {}^\ell G^d$ and the ratio of s to d disconnected quark loops is denoted by ${}^\ell R_d^s = {}^\ell G^s / {}^\ell G^d$.

Rearranging Eqs. (1), (2) and (4) to isolate the strange quark loop contribution ${}^\ell G^s$ yields two independent expressions which are direct consequences of QCD under the assumption of charge symmetry:

$$^\ell G^s = \left(\frac{{}^\ell R_d^s}{1 - {}^\ell R_d^s} \right) [2p + n - u^p], \qquad (5)$$

$$^\ell G^s = \left(\frac{{}^\ell R_d^s}{1 - {}^\ell R_d^s} \right) [p + 2n - d^p]. \qquad (6)$$

In principle, given a suitable estimate of ${}^\ell R_d^s$, these expressions may be simply evaluated; the total form factors p and n are well known experimentally and the connected contributions u^p and u^n may be calculated on the lattice.

This procedure relies on the assumption that the difference between the experimental numbers and the connected lattice simulation results for the form factors may be entirely attributed to contributions from disconnected quark loops, i.e., that all other systematic effects are under control. To allow for any as-yet undetermined lattice systematics, we average Eqs. (5) and (6) resulting in a form where only the connected contribution to the combination $(u^p + d^p)$ needs to be determined from the lattice:

$$^\ell G^s = \left(\frac{{}^\ell R_d^s}{1 - {}^\ell R_d^s} \right) \left[\frac{3}{2}(p + n) - \frac{1}{2}(u^p + d^p)_{\text{Latt.}} \right]. \qquad (7)$$

As will be described in Sec. 2.1, the additional systematic uncertainty on $(u^p + d^p)$ is approximated by that on the isovector combination $(u^p - d^p)$. The latter may be determined by direct comparison with experiment as contributions from disconnected u and d loops are equal and hence cancel.

In the following sections we discuss each of the three inputs into Eq. (7):

- The lattice values for $(u^p + d^p)$.

- The experimental p and n form factors.

- The ratio ${}^\ell R_d^s = {}^\ell G^s / {}^\ell G^d$.

2.1. Lattice determination of u^p and d^p

Lattice values for the connected u and d quark contributions to the proton electric and magnetic form factors, u^p and d^p, are taken from Refs. [26, 27]. As discussed above, we include an additional systematic uncertainty on these results in addition to that quoted in the original papers.

We estimate that the unaccounted-for systematic uncertainty of $(u^p + d^p)$ will be similar to that of the isovector combination $(u^p - d^p)$. As the latter should agree with experiment if all systematic effects are under control (recalling that disconnected contributions cancel in this combination), the difference between lattice and experimental results $(u^p - d^p)_{\text{Latt.}} - (p - n)_{\text{Exp.}}$ provides an estimate of the remaining uncertainty. We take the largest value of this difference, evaluated at the six simulation values of Q^2, as a conservative estimate. The experimental numbers for the form factors p and n are taken from the Kelly [32] or Arrington and Sick [33] parameterisations. Section 2.2 gives details of the way in which the results using each parameterisation are combined.

This procedure is followed for both the electric and magnetic form factors. As will be illustrated in Table 1 in Sec. 4, the additional uncertainty included in
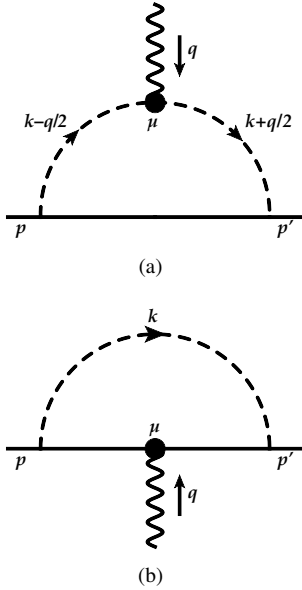
Figure 1: Loop diagrams which are included in the estimate of $^\ell R_d^s$ from effective field theory. Fig. 1(b) is included for the electric form factor only. The solid, dashed and wavy lines denote octet baryons, mesons and photons respectively.
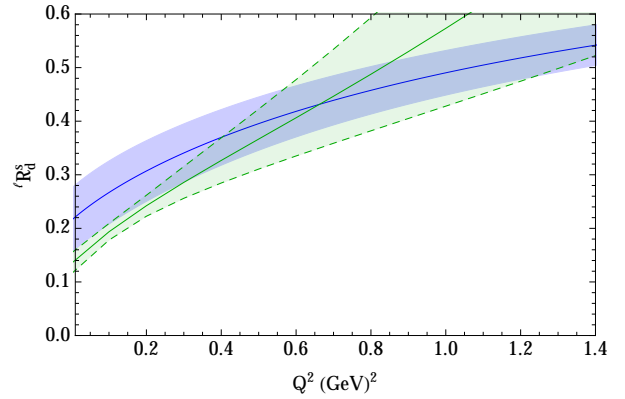

Figure 2: Estimate of $^\ell R_d^s$ from effective field theory with finite-range regularisation for the electric (dashed green) and magnetic (solid blue) form factors.

this fashion is significant and larger than the statistical uncertainty in the determination of the strange magnetic form factor. For the electric form factor it is a modest contribution of a size similar to or smaller than the statistical uncertainty.

2.2. Experimental p and n form factors

The experimental proton and neutron electromagnetic form factors p and n are taken from the parameterisations of experimental results by Kelly [32] and Arrington and Sick [33] (the latter is used only on its quoted range of validity, $Q^2 < 1$ GeV^2). The entire calculation, including the additional estimate of lattice systematics described in Sec. 2.1, is performed using each parameterisation. The average central value of the two sets of results is taken as the best-estimate of the strange form factors. Half of the difference between the two central values is included as an estimate of the parameterisation-dependent uncertainty. As shown in Table 1 in Sec. 4, this contribution to the uncertainty is small.

2.3. Estimate of the ratio $^\ell R_d^s$

We derive an estimate for the disconnected quark-loop ratio $^\ell R_d^s = {}^\ell G^s / {}^\ell G^d$ using a model based on chiral effective field theory, as also done in Refs. [23–25]. In

that formalism $^\ell R_d^s$ is given by the ratio of loop diagram contributions to the electromagnetic form factors, where the relevant loop integrals are weighted by the appropriate 'disconnected' chiral coefficients for the s and d quarks [24, 25, 28].

The primary loop diagram relevant to this calculation is illustrated in Fig. 1(a). For the electric form factor, in particular, a higher-order diagram (Fig. 1(b)) is important as it makes a significant contribution of the opposite sign to that of Fig. 1(a), resulting in a large cancellation. While to the order of the calculation in Refs. [26, 27] this term contributes a constant to $G_E(Q^2)$ (enforcing charge conservation at $Q^2 = 0$), this is not a good approximation for the large Q^2 values considered in this work.

For this reason we include Fig. 1(b), with an estimate of its Q^2-dependence, explicitly in our calculation of $^\ell R_d^s$ for the electric form factor. This is achieved by calculating the diagram in heavy-baryon chiral perturbation theory and modelling the Q^2-dependence of the photon-baryon vertex based on the lattice results of Ref. [26]. Further details are given in Appendix A.

For both the electric and magnetic form factors the effect of additionally including loops with decuplet baryon intermediate states is taken as an estimate of the uncertainty in the ratio $^\ell R_d^s$. The errors quoted for the numerical results in Table 1 in Sec. 4 combine this estimate in quadrature with that given by allowing the dipole mass parameter Λ used in the finite-range regularisation scheme to vary between 0.6 and 1.0 GeV. That regularisation procedure is discussed in Refs. [34–36]. The final values for $^\ell R_d^s$ are shown in Fig. 2.

3

3. Strange magnetic moment $G_M^s(Q^2 = 0)$

For the magnetic form factor at $Q^2 = 0$ there is additional information available from experiment as the hyperon magnetic moments have been measured [37]. We rearrange Eqs. (5) and (6), using the assumption of charge symmetry, to express the strange magnetic moment in terms of the hyperon moments [22, 31]:

$$^\ell G^s = \left(\frac{^\ell R_d^s}{1 - {}^\ell R_d^s}\right)\left[2p + n - \frac{u^p}{u^\Sigma}\left(\Sigma^+ - \Sigma^-\right)\right], \quad (8)$$

$$^\ell G^s = \left(\frac{^\ell R_d^s}{1 - {}^\ell R_d^s}\right)\left[p + 2n - \frac{u^n}{u^\Xi}\left(\Xi^0 - \Xi^-\right)\right]. \quad (9)$$

This rearrangement minimises the propagation of lattice systematics as only ratios of form factors must be determined from lattice QCD. Of course, as the hyperon form factors have not been determined experimentally at non-zero values of Q^2, these expressions can at this stage only be used at $Q^2 = 0$.

The ratios u_M^p/u_M^Σ and u_M^n/u_M^Ξ of up quark contributions to the hyperon form factors, at a range of non-zero values of the momentum transfer Q^2, are taken from Refs. [26, 27] (raw results are given in Appendix A of Ref. [27]). We determine the $Q^2 = 0$ values needed here using a linear extrapolation in Q^2, with an additional experimental constraint provided by the equality of Eqs. (8) and (9):

$$\frac{u_M^p}{u_M^\Sigma} = \frac{u_M^n}{u_M^\Xi}\left(\frac{\mu_{\Xi^0} - \mu_{\Xi^-}}{\mu_{\Sigma^+} - \mu_{\Sigma^-}}\right) + \left(\frac{\mu_p - \mu_n}{\mu_{\Sigma^+} - \mu_{\Sigma^-}}\right), \quad (10)$$

where μ_B denotes the experimental magnetic moment of the baryon B [37]. This extrapolation is illustrated in Fig. 3. The fit is performed to the lattice results where $Q^2 < 1$ GeV^2, which display qualitatively linear behaviour and for which the linear-fit χ^2/d.o.f is acceptable given the constraint of Eq. (10). Fitting to one less data point does not change the results appreciably, as also illustrated in Fig. 3.

The best estimates of the $Q^2 = 0$ ratios of connected contributions to the baryon magnetic form factors are

$$\frac{u_M^p}{u_M^\Sigma} = 1.096 \pm 0.016 \quad \text{and} \quad \frac{u_M^n}{u_M^\Xi} = 1.239 \pm 0.090. \tag{11}$$

These numbers align remarkably well with those determined in Ref. [23] using quenched lattice simulation results (after the application of a theoretical 'unquenching' formalism [35]). The resulting value for the strange magnetic moment (from Eqs. (8) and (9)), conventionally defined without the charge factor, is
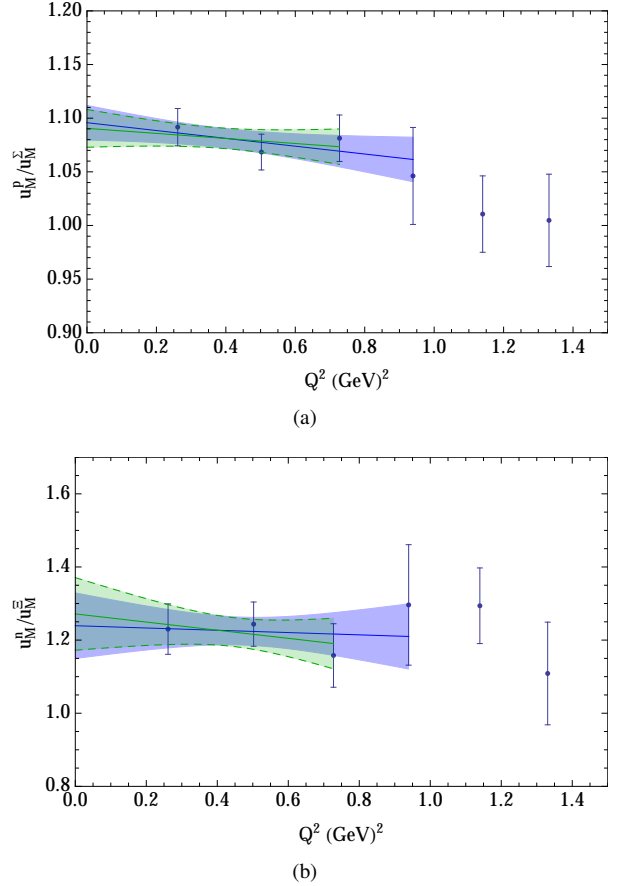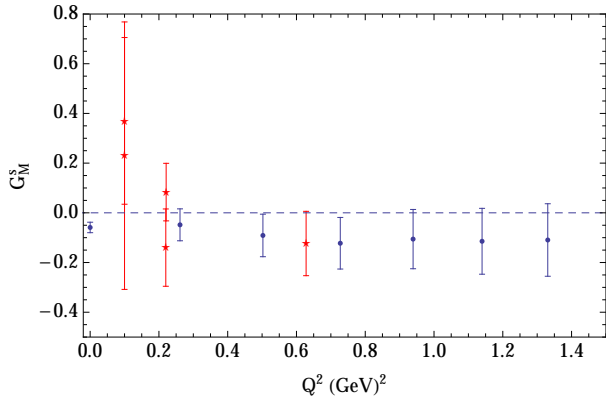
$$G_M^s(Q^2 = 0) = -0.07 \pm 0.03\,\mu_N. \tag{12}$$

(a)

(b)

Figure 3: Results from Refs. [26, 27] for the ratios u_M^p/u_M^Σ and u_M^n/u_M^Ξ of connected contributions to the baryon magnetic form factors. The bands show simultaneous fits, linear in Q^2, to the lowest 4 (blue solid band) or 3 (green dashed band) data points, constrained by Eq. (10) at $Q^2 = 0$.

4

(a) Strange magnetic form factor of the proton in units of nuclear magnetons (μ_N).
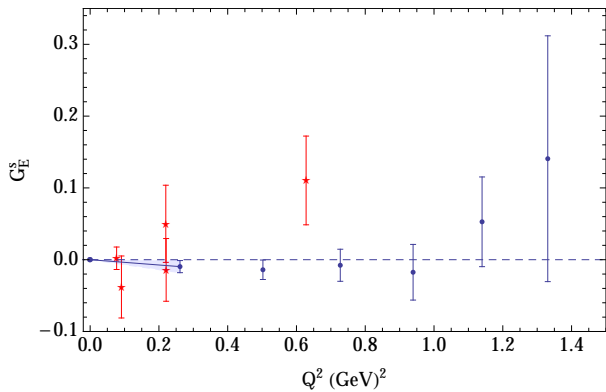
(b) Strange electric form factor of the proton. The blue band indicates a straight-line fit in Q^2 to the lowest-Q^2 point, which we use to estimate the strange electric charge radius.

Figure 4: Strange contribution to the electromagnetic form factors of the proton, for strange quarks of unit charge. The experimental results (red stars) are taken from Refs. [2, 4, 5, 8, 9, 12].

The uncertainties are dominated by that in the ratio $^{\ell}R_d^s$ (see Sec. 2.3); more explicitly $G_M^s(Q^2 = 0) = -0.071 \pm 0.013 \pm 0.025 \pm 0.004 \, \mu_N$ where the first uncertainty is propagated from the lattice simulation results, the second contribution comes from the ratio $^{\ell}R_d^s$ and the last is that from the experimental determination of the magnetic moments [37].

4. Results at finite Q^2

The results of this analysis for the strange electric and magnetic form factors of the proton at six discrete nonzero values of the momentum transfer Q^2, and additionally at $Q^2 = 0$ for the magnetic case, are displayed in Fig. 4 alongside the latest experimental determinations of those quantities. All results away from $Q^2 = 0$ are
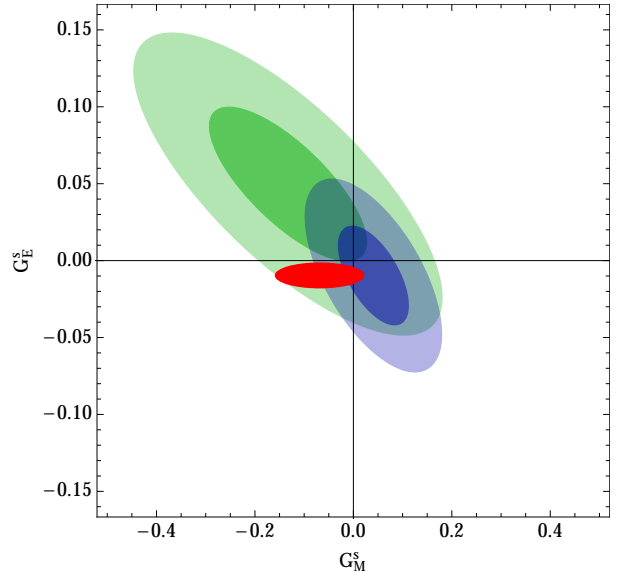

Figure 5: Comparison of the results of this work (red ellipse) at $Q^2 = 0.26$ GeV^2 with available experimental results at similar values of Q^2. The dark and pale green ellipses show 1σ and 2σ results from the A4 Collaboration at $Q^2 = 0.23$ GeV^2 [11] while the blue ellipses show G0 Collaboration results close to $Q^2 = 0.23$ GeV^2 [1, 2].

consistent with zero to within 2-sigma. The results for the strange magnetic form factor favour negative values which are consistent with recent experimental results.

Since experimental determinations of the strange form factors are obtained as linear combinations of G_E^s and G_M^s we also display results at the lowest value of the momentum transfer, $Q^2 = 0.26$ GeV^2, in the G_M^s–G_E^s plane in Fig. 5. The available experimental results for similar values of Q^2 appear on this figure as ellipses. The present calculation is consistent with experiment to within 2-sigma. Numerical results, including a breakdown of the systematic uncertainties in the calculation, are given in Table 1.

One can also use the results of this analysis to estimate the strange electric charge radius of the proton. We perform a simple calculation using a straight-line fit in Q^2 to the lowest-Q^2 result for G_E^s (illustrated in Fig. 4(b)). This gives $\langle r_E^2 \rangle^s = 0.0086 \pm 0.0043 \pm 0.0066$ fm^2, where the first uncertainty is statistical and the second systematic (including in quadrature all systematic uncertainties of Table 1). This is consistent with the results of Ref. [25] obtained using quenched lattice simulations. We note that fits including the lowest 2, 3 or 4 points in Q^2 all yield results with uncertainties contained entirely within the quoted range.

Finally, we report that the most precise result of this

Q^2 (GeV^2)	G_M^s (μ_N)	G_E^s
0.26	−0.069(12)(44)(15)(78)	−0.010(4)(5)(2)(6)
0.50	−0.109(12)(59)(21)(112)	−0.014(8)(8)(3)(7)
0.73	−0.136(15)(72)(24)(129)	−0.008(15)(11)(1)(13)
0.94	−0.122(20)(83)(20)(136)	−0.017(28)(16)(3)(20)
1.14	−0.103(16)(94)(17)(137)	0.053(34)(24)(40)(24)
1.33	−0.115(20)(103)(18)(135)	0.141(57)(35)(153)(36)

Table 1: Results for the strange electric and magnetic form factors of the proton at the six non-zero values of Q^2 investigated here. The first uncertainty quoted comes from the lattice values for the connected u and d quark contributions to the proton form factors, taken from Refs. [26, 27], while the second is the additional systematic uncertainty included as described in Sec. 2.1. The third uncertainty is that propagated from the factor $\left({}^\ell R_d^s / (1 - {}^\ell R_d^s) \right)$ (see Sec. 2.3). The last uncertainty is that from the Kelly parameterisation of the experimental p and n form factors [32], combined in quadrature with the parameterisation uncertainty in those results for $Q^2 < 1$ where we use two parameterisations as described in Sec. 2.2.

analysis is that for the strange magnetic moment of the proton: $G_M^s(Q^2 = 0) = -0.07 \pm 0.03\,\mu_N$. This number is non-zero to 2-sigma and an order of magnitude more precise than the closest experimental results.

Acknowledgements

Appendix A. Details of the calculation of ${}^\ell R_d^s$

In this section we give further details of the calculation of the ratio of disconnected loop contributions, ${}^\ell R_d^s = {}^\ell G^s / {}^\ell G^d$, described in Sec. 2.3.

The loop diagram shown in Fig. 1(a) gives contributions to the magnetic and electric form factors of the proton which depend on the integrals I_M and I_E respec-

tively:

$$I_M(m, Q^2) = \int d\vec{k}\, \frac{k_y^2 u(\vec{k} + \vec{q}/2) u(\vec{k} - \vec{q}/2)}{2\omega_+^2 \omega_-^2}, \qquad (A.1)$$

$$I_E(m, Q^2) = \int d\vec{k}\, \frac{(\vec{k}^2 - \vec{q}^2/4) u(\vec{k} + \vec{q}/2) u(\vec{k} - \vec{q}/2)}{\omega_+ \omega_- (\omega_+ + \omega_-)}, \qquad (A.2)$$

where

$$\omega_\pm = \sqrt{(\vec{k} \pm \vec{q}/2)^2 + m^2}, \qquad (A.3)$$

$\vec{q}$ is defined to lie along the z-axis, $Q^2 = -q^2$ and $u(\vec{k})$ is the ultra-violet regulator used in the finite-range regularization scheme. As was done for the chiral extrapolation of the lattice results used in this calculation [26, 27], we choose a dipole regulator $u(k) = \left(\frac{\Lambda^2}{\Lambda^2 + k^2} \right)^2$ with a regulator mass $\Lambda = 0.8 \pm 0.2$ GeV. The dipole form is suggested by a comparison of the nucleon's axial and induced pseudoscalar form factors [41] and the choice of Λ is informed by a lattice analysis of nucleon magnetic moments [42].

For the electric form factor we also consider Fig. 1(b), as discussed in Sec. 2.3. In the formalism used here, this diagram contributes a constant to the electric form factor which is equal in magnitude and opposite in sign to the contribution from Fig. 1(a) at $Q^2 = 0$, ensuring that the electric charge remains unrenormalised. We model the Q^2-dependence of Fig. 1(b) by scaling that constant by an appropriate form factor. This results in a contribution to G_E which is identical to that of Fig. 1(a) under the replacement

$$I_E(m_\phi, Q^2) \to -I_E(m_\phi, 0) * G_E^q(Q^2). \qquad (A.4)$$

Here G_E^q (for $q = \{d, s\}$) is the q quark contribution to the 'intermediate' baryon form factor; it is the average

contribution of q quarks to the form factors of the intermediate baryons in the loop with a proton external state, weighted by the appropriate Clebsch-Gordon coefficients. We approximate this for the s quark by the form factor $G_E^{\Sigma^0,s}$, taken from Ref. [26]. Similarly, we set G_E^d to the same quantity, but where the strange quark mass is set equal to the light quark mass in the chiral extrapolation of Ref. [26].

The contributions of the loop diagrams of Fig. 1 to the proton electric and magnetic form factors are given by the loop integrals defined above, weighted by the appropriate chiral coefficients. As the *disconnected* chiral coefficients for the d and s quarks are the same (and cancel in the ratio), the central values of ${}^\ell R_d^s$ at each Q^2 are given simply by the ratio of the integrals $I(m_\phi, Q^2)$ with pion and kaon masses in the loops:

$$ {}^\ell R_{dM}^s(Q^2) = \frac{I_M(m_\pi, Q^2)}{I_M(m_K, Q^2)}, \tag{A.5} $$

$$ {}^\ell R_{dE}^s(Q^2) = \frac{I_E(m_\pi, Q^2) - I_E(m_\pi, 0) * G_E^d(Q^2)}{I_E(m_K, Q^2) - I_E(m_K, 0) * G_E^s(Q^2)}. \tag{A.6} $$

The dominant uncertainty in ${}^\ell R_d^s$ comes from allowing the regulator mass Λ to vary in the range 0.6-1.0 GeV. This is combined in quadrature with half of the shift that results from additionally allowing decuplet intermediate states in the loops. The calculation including the decuplet loops proceeds as described above, with additional terms of the relevant decuplet-intermediate-state loop integrals (given in Refs. [26, 27]) in both the numerator and denominator of Eqs. A.5 and A.6, weighted by the appropriate relative disconnected chiral coefficients which may be found in Ref. [24].

References

References

[1] D. Armstrong, et al., Strange quark contributions to parity-violating asymmetries in the forward G0 electron-proton scattering experiment, Phys.Rev.Lett. 95 (2005) 092001.

[2] D. Androić, et al., Strange Quark Contributions to Parity-Violating Asymmetries in the Backward Angle G0 Electron Scattering Experiment, Phys.Rev.Lett. 104 (2010) 012001.

[3] K. Aniol, et al., Constraints on the nucleon strange form-factors at $Q^2 \sim 0.1$ GeV^2, Phys.Lett. B635 (2006) 275–279.

[4] K. Aniol, et al., Parity-violating electron scattering from He-4 and the strange electric form-factor of the nucleon, Phys.Rev.Lett. 96 (2006) 022003.

[5] A. Acha, et al., Precision Measurements of the Nucleon Strange Form Factors at $Q^2 \sim 0.1$ GeV^2, Phys.Rev.Lett. 98 (2007) 032301.

[6] Z. Ahmed, et al., New precision limit on the strange vector form factors of the proton, Phys. Rev. Lett. 108 (2012) 102001.

[7] K. A. Aniol, et al., Parity-violating electroweak asymmetry in $\vec{e}p$ scattering, Phys. Rev. C 69 (2004) 065501.

[8] D. T. Spayde, et al., The strange quark contribution to the proton's magnetic moment, Physics Letters B 583 (2004) 79 – 86.

[9] E. Beise, M. Pitt, D. Spayde, The SAMPLE experiment and weak nucleon structure, Prog.Part.Nucl.Phys. 54 (2005) 289–350.

[10] F. E. Maas, et al., Evidence for strange quark contributions to the nucleon's form-factors at $q^2 = 0.108$ (GeV/c)^2, Phys.Rev.Lett. 94 (2005) 152001.

[11] F. E. Maas, et al., Measurement of strange quark contributions to the nucleon's form-factors at $Q^2 = 0.230$ (GeV/c)^2, Phys.Rev.Lett. 93 (2004) 022002.

[12] S. Baunack, et al., Measurement of Strange Quark Contributions to the Vector Form Factors of the Proton at $Q^2 = 0.22$ (GeV/c)^2, Phys.Rev.Lett. 102 (2009) 151803.

[13] R. D. Young, J. Roche, R. D. Carlini, A. W. Thomas, Extracting nucleon strange and anapole form factors from world data, Phys.Rev.Lett. 97 (2006) 102002.

[14] B. S. Zou, D. O. Riska, $s\bar{s}$ component of the proton and the strangeness magnetic moment, Phys. Rev. Lett. 95 (2005) 072001.

[15] R. L. Jaffe, Stranger than fiction: The strangeness radius and magnetic moment of the nucleon, Physics Letters B 229 (1989) 275 – 279.

[16] H.-W. Hammer, U.-G. Meißner, D. Drechsel, The strangeness radius and magnetic moment of the nucleon revisited, Physics Letters B 367 (1996) 323 – 328.

[17] T. D. Cohen, H. Forkel, M. Nielsen, Just how strange? loops, poles and the strangeness radius of the nucleon, Physics Letters B 316 (1993) 1 – 6.

[18] N. W. Park, J. Schechter, H. Weigel, Electromagnetic, axial-vector, and strange currents in the skyrme model: Effects of symmetry breaking, Phys. Rev. D43 (1991) 869–884.

[19] H. Weigel, A. Abada, R. Alkofer, H. Reinhardt, On the strange vector form factors of the nucleon in the {NJL} soliton model, Physics Letters B 353 (1995) 20 – 26.

[20] A. Abdel-Rehim, et al., Disconnected quark loop contributions to nucleon observables in lattice QCD, Phys.Rev. D89 (2014) 034501.

[21] T. Doi, et al., Nucleon strangeness form factors from N(f) = 2+1 clover fermion lattice QCD, Phys.Rev. D80 (2009) 094503.

[22] D. B. Leinweber, QCD equalities for baryon current matrix elements, Phys.Rev. D53 (1996) 5115–5124.

[23] D. B. Leinweber, et al., Precise determination of the strangeness magnetic moment of the nucleon, Phys.Rev.Lett. 94 (2005) 212001.

[24] P. Wang, D. B. Leinweber, A. W. Thomas, R. D. Young, Strange magnetic form factor of the proton at $Q^2 = 0.23$ GeV^2, Phys.Rev. C79 (2009) 065202.

[25] D. B. Leinweber, et al., Strange electric form-factor of the proton, Phys.Rev.Lett. 97 (2006) 022001.

[26] P. E. Shanahan, et al., Electric form factors of the octet baryons from lattice QCD and chiral extrapolation, arXiv:1403.1965 (2014).

[27] P. E. Shanahan, et al., Magnetic form factors of the octet baryons from lattice QCD and chiral extrapolation, arXiv:1401.5862 (2014).

[28] D. B. Leinweber, Quark contributions to baryon magnetic moments in full, quenched and partially quenched QCD, Phys.Rev. D69 (2004) 014005.

[29] B. C. Tiburzi, Connected Parts of Decuplet Electromagnetic Properties, Phys.Rev. D79 (2009) 077501.

[30] D. B. Leinweber, Not strange but bizarre physics from the sample experiment (1998) 121–130.

[31] D. B. Leinweber, A. W. Thomas, A Lattice QCD analysis of the strangeness magnetic moment of the nucleon, Phys.Rev. D62 (2000) 074505.

[32] J. J. Kelly, Simple parametrization of nucleon form factors, Phys.Rev. C70 (2004) 068202.

[33] J. Arrington, I. Sick, Precise determination of low-Q nucleon electromagnetic form factors and their impact on parity-violating e-p elastic scattering, Phys.Rev. C76 (2007) 035201.

[34] D. B. Leinweber, A. W. Thomas, R. D. Young, Physical nucleon properties from lattice QCD, Phys.Rev.Lett. 92 (2004) 242002.

[35] R. D. Young, D. B. Leinweber, A. W. Thomas, S. V. Wright, Chiral analysis of quenched baryon masses, Phys.Rev. D66 (2002) 094507.

[36] R. D. Young, D. B. Leinweber, A. W. Thomas, Convergence of chiral effective field theory, Prog.Part.Nucl.Phys. 50 (2003) 399–417.

[37] J. Beringer, et al., Phys.Rev. D86 (2012).

[38] Y. Nakamura, H. Stüben, BQCD - Berlin quantum chromodynamics program, PoS LATTICE2010 (2010) 040.

[39] P. A. Boyle, The BAGEL assembler generation library, Comput.Phys.Commun. 180 (2009) 2739–2748.

[40] R. G. Edwards, B. Joo, The Chroma software system for lattice QCD, Nucl.Phys.Proc.Suppl. 140 (2005) 832.

[41] P. A. M. Guichon, G. A. Miller, A. W. Thomas, The Axial Form-factor of the Nucleon and the Pion - Nucleon Vertex Function, Phys.Lett. B124 (1983) 109.

[42] J. M. M. Hall, D. B. Leinweber, R. D. Young, Chiral extrapolations for nucleon magnetic moments, Phys.Rev. D85 (2012) 094502.